JOURNAL OF MAGNETIC RESONANCE **135,** 227–231 (1998)
ARTICLE NO. MN981544

COMMUNICATIONS

Orientational Constraints Derived from Hydrated Powder Samples by Two-Dimensional PISEMA

F. Tian, Z. Song, and T. A. Cross

Department of Chemistry, Center for Interdisciplinary Magnetic Resonance, National High Magnetic Field Laboratory, Institute of Molecular Biophysics, Florida State University, Tallahassee, Florida 32310

Received April 10, 1998; revised May 29, 1998

Axial rotation causes the chemical shift and dipolar tensors to be collinear (*1, 2*). Powder pattern spectra of molecules having axial rotation can yield orientational constraints without the need for orienting the sample. Furthermore, the relative orientation of chemical shift and dipolar interaction tensors in the principle axis system (PAS) frame of reference can be constrained through 2D spectra. Here PISEMA (*p*olarization *i*nversion *s*pin *e*xchange at *m*agic *a*ngle) (*3*) spectra of the polypeptide gramicidin A are presented to illustrate the quality of the constraints obtainable in this way and the potential interpretation of such data.

Orientational dependent nuclear spin interactions from solid-state NMR can be used to determine the orientation, internal dynamics, and three-dimensional structure of membrane-associated proteins or peptides (*4*). Constraints from uniformly aligned preparations have been successfully applied to define the high-resolution three-dimensional structure of a polypeptide, gramicidin A, in an anisotropic lipid bilayer environment (*5–7*). While this structure was based on specific site isotopic labeling, well resolved 2D or 3D spectra of uniformly ^{15}N-labeled membrane proteins from 50 to 200 residues in oriented phospholipid bilayers have been obtained through PISEMA experiments (*8–10*).

The preparation of macroscopically aligned membrane and membrane-associated proteins is one of the challenging prerequisites for this structure determination approach. Considerable efforts have gone into the development of methods for orienting samples (*11–13*). Uniformly aligned samples are generally prepared in one of two ways: mechanically aligned lipid bilayers by shearing samples between two glass plates (*11*), or magnetically aligned bilayer-like disks called bicelles (*14*). A major disadvantage of the mechanical alignment is that most of the sample volume is occupied by glass which results in a loss of sensitivity (*13*). The addition of small amounts of lanthanide ions, such as En^{3+}, Er^{3+}, Tm^{3+}, and Yb^{3+} has been shown to flip the aligned bicelles by 90° with respect to the magnetic field, bringing the bilayer normal parallel to the magnetic field (*15*). However, numerous concerns about these preparations need to be addressed before high-resolution structural constraints can be obtained.

In this communication, we will demonstrate that high-resolution structural constraints can also be obtained from unoriented samples in which rapid rotational diffusion occurs about at least one axis. This may be true for many membrane bound polypeptides and small proteins and is true for the polypeptide channel, gramicidin A, in hydrated lipid bilayers. With the 2D PISEMA pulse sequence, the spectral resolution from an unoriented, single site labeled "powder" sample is comparable with the resolution obtained from oriented samples. Thus, the tedious preparation of oriented samples could be avoided.

The PISEMA pulse sequence is based on the previously established frequency switched Lee-Goldburg (FSLG-2) homonuclear decoupling pulse sequence (*16–18*). PISEMA can be used to obtain two-dimensional ^{15}N chemical shift/^{15}N-^{1}H dipolar correlation spectra with much improved resolution in the dipolar dimension, as compared to *s*eparated *l*ocal *f*ield (SLF) experiments (*19*). In the PISEMA pulse sequence, cross-polarization (CP) is followed by spin exchange at the magic angle, in which the I spins (^{1}H) are locked along the magic angle, 54.7°, with respect to the external field, B_0, and the S spins (^{15}N) are locked in the transverse plane by an effective field matched with that for the I spins. Therefore, the homonuclear I–I dipolar interactions are suppressed and the magnetization oscillation between I and S spins is mediated by the scaled (0.82) heteronuclear dipolar coupling. The tilted field is produced by RF irradiation offset from resonance according to LG conditions, $\Delta\omega = \pm\omega_{1I}/\tan(54.7°)$. The FSLG cycles are incremented in steps which correspond to the t_1 dwell time. As a result, the linewidth in the dipolar dimension is governed by the $T_{1\rho}$ of the I spins.

In samples with axial rotational diffusion faster than the NMR spin interaction time scale, the asymmetric chemical-shift powder pattern will be averaged to a symmetric tensor with the motionally averaged chemical-shift interaction, $\sigma_{\parallel}$,

$$\sigma_{\parallel} = \sigma_{11}\mathrm{Cos}^2\zeta\ \mathrm{Sin}^2\xi + \sigma_{22}\mathrm{Sin}^2\zeta\ \mathrm{Sin}^2\xi + \sigma_{33}\mathrm{Cos}^2\xi,$$

where ζ and ξ are the polar angles defining the motional axis,

1090-7807/98 $25.00

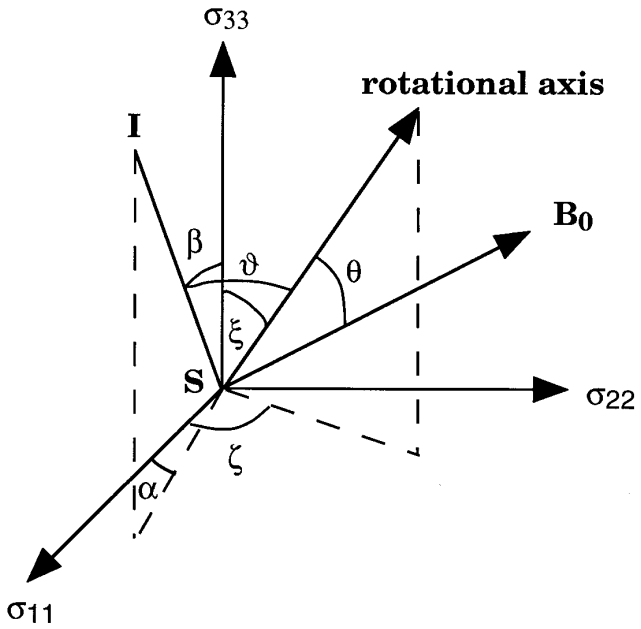

FIG. 1. Definition of the rotational axis and the I-S internuclear vector with respect to the chemical-shift PAS frame.

i.e., the channel axis, in the chemical-shift PAS frame (Fig. 1). Each position in the powder pattern (σ_{obs}) corresponds to molecules whose rotational axes make a particular angle θ with respect to the external magnetic field,

$$\sigma_{obs} = \frac{1}{2}\sigma_{\parallel}(3\ \mathrm{Cos}^2\theta - 1) \qquad [1]$$

with the average of the tensor elements, $\sigma_{iso} = 0$. The observed dipolar interaction of any isolated pair of spin $\frac{1}{2}$ nuclei from such a randomly oriented sample can be calculated as

$$\Delta\nu_{obs} = \pm\frac{R}{2}(3\ \mathrm{Cos}^2\vartheta - 1)\cdot(3\ \mathrm{Cos}^2\theta - 1), \qquad [2]$$

where ϑ is the angle between the internuclear vector and the rotational (channel) axis, and R is the dipolar coupling constant, $R = (\mu_0/4\pi)(\gamma_I\gamma_S h/2\pi r_{IS}^3)$. Here γ is gyromagnetic ratio, h Planck's constant, and r the distance between I and S spins. Moreover,

$$\mathrm{Cos}\vartheta = \mathrm{Cos}\beta\mathrm{Cos}\xi + \mathrm{Sin}\alpha\mathrm{Sin}\beta\mathrm{Sin}\zeta\mathrm{Sin}\xi + \mathrm{Cos}\alpha\mathrm{Sin}\beta\mathrm{Cos}\zeta\mathrm{Sin}\xi, \qquad [3]$$

where α and β define the orientation of the internuclear vector in the PAS frame (Fig. 1). Since θ determines both observations, σ_{obs} and $\Delta\nu_{obs}$, combining Eqs. [1] and [2] gives

$$\Delta\nu_{obs} = \pm R(3\ \mathrm{Cos}^2\vartheta - 1)\cdot\frac{\sigma_{obs}}{\sigma_{\parallel}}. \qquad [4]$$

Equation [4] suggests that the observed dipolar interaction should vary linearly with the chemical shift across the powder pattern. A contour plot of the 2D dipolar/chemical shift spectra should yield two lines crossing at the isotropic chemical shift, where the rotational axis is oriented at 54.7° with respect to the magnetic field direction. The slope of the line is related to the orientation of the internuclear vector with respect to the rotational axis and, by Eq. [3], related to α and β, that orient the dipolar and chemical-shift tensors relative to each other.

Gramicidin A (gA) is a 15-amino acid polypeptide which forms a cation channel across membranes (*20, 21*). The transmembrane form is a dimer where each monomer is a single-stranded right-handed β helix with 6.5 residues per turn (PDB: 1MAG). The rotational diffusion of gramicidin A about the channel axis which is parallel to the lipid bilayer normal has been extensively characterized by ^{2}H NMR (*22, 23*). At 278 K, the global rotation is frozen out, thus the asymmetric ^{15}N chemical-shift powder pattern ($\eta = 0.23$) is observed, as shown in Fig. 2A. When the temperature is raised to 298 K, approximately the temperature of the lipid phase transition, the symmetric ^{15}N chemical-shift powder lineshape is obtained as a result of fast global motion about the channel axis (Fig. 2B).

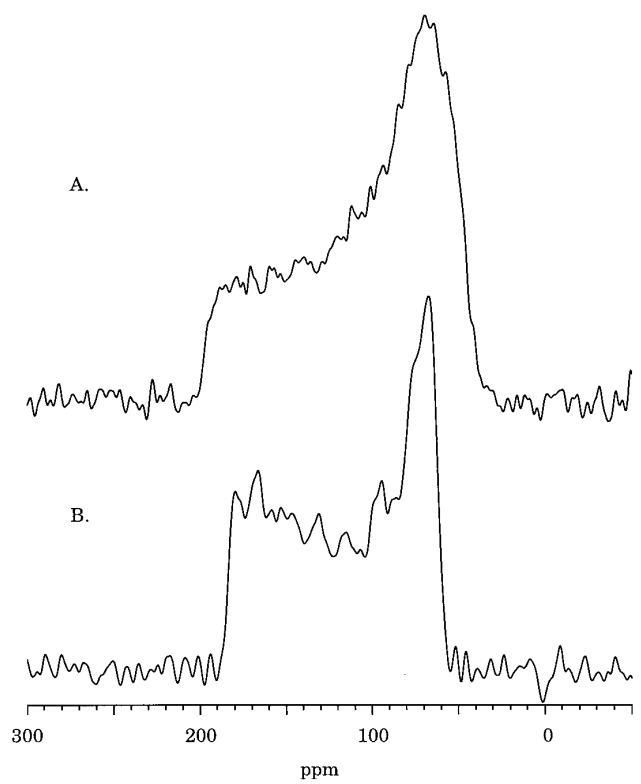

FIG. 2. ^{15}N chemical-shift powder pattern spectra for ^{15}N-Trp$_{13}$ gramicidin A in hydrated DMPC bilayers. (A) At 278 K, the global rotation is frozen out (correlation time of the global motion is ≥33 ms), and consequently, the asymmetric chemical-shift powder pattern is obtained. (B) At 298 K, the rotational diffusion around the channel axis results in a symmetric chemical-shift lineshape (correlation time of the global motion is ~3.3 μs).

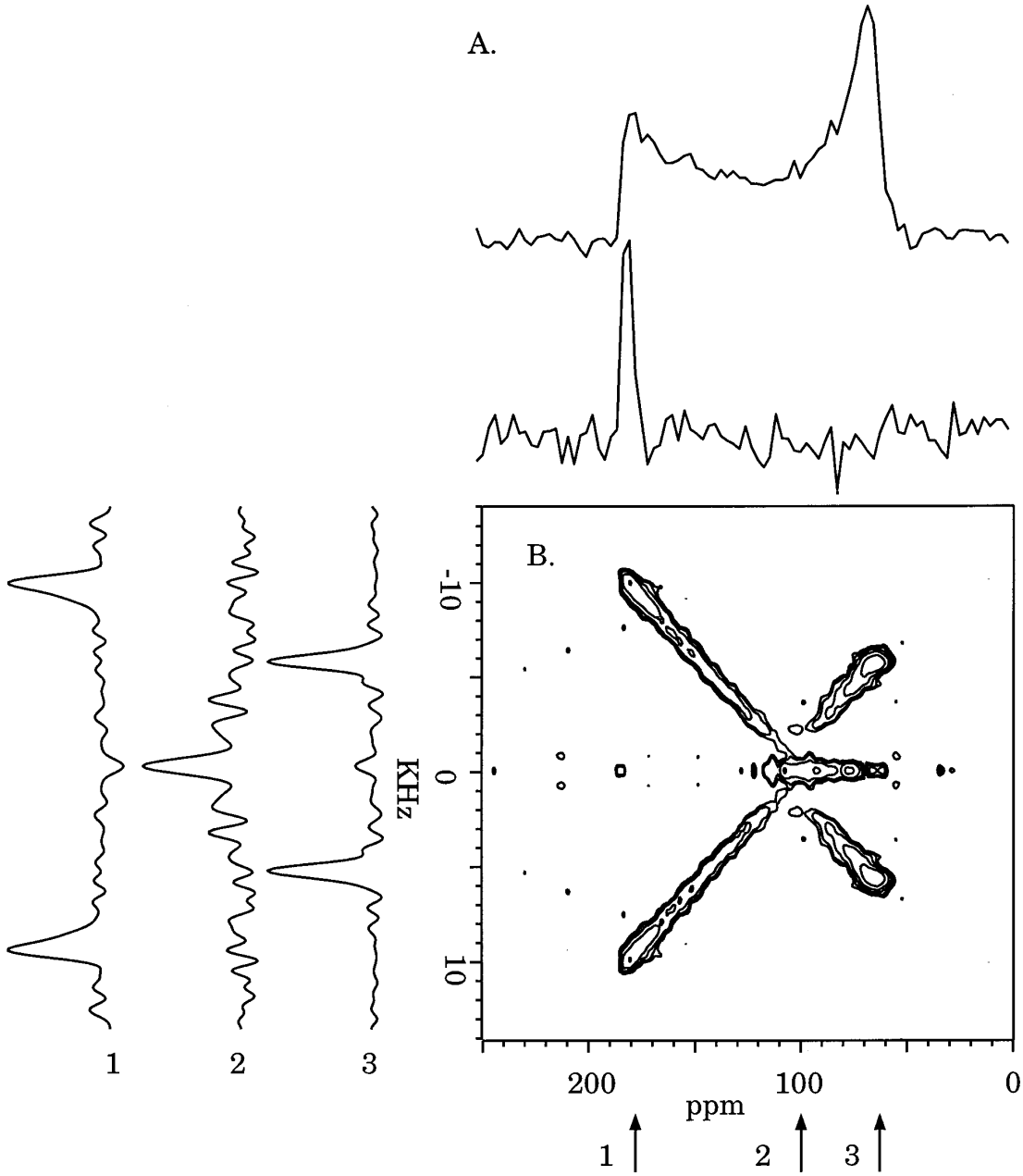

FIG. 3. PISEMA spectra of 60 mg ^{15}N-Trp$_{13}$ gramicidin A in hydrated unoriented DMPC bilayers (1:8 peptide/lipid molar ratio) at 298 K. (A) The 1D ^{15}N chemical-shift powder pattern projection. (B) Contour plot of 2D spectra shows the chemical-shift anisotropy along the horizontal axis and the dipolar splitting along the vertical axis. On the left, slices are taken along the dipolar dimension corresponding to arrows 1, 2, 3. The spectrum above the contour plot is the ^{15}N chemical shift from the maximal dipolar splitting. The spectra were recorded on a homebuilt 400-MHz triple resonance spectrometer assembled around a Chemagnetics data acquisition system. The RF field strength of 48.6 kHz was used on the ^{1}H channel and a frequency jump of 34.4 kHz set the Lee–Goldburg homonuclear decoupling condition during the spin exchange period. The RF field on the ^{15}N channel fulfilled the Hartmann–Hahn match at 59.5 kHz during t_1. There were 512 points acquired in t_2, and 1600 transients were coadded for each of 32 t_1 experiments with a dwell time of 43 μs. The recycle delay was 3 s. The frequency and phase switch time of our spectrometer is on the order of tens of nanoseconds; however, the rise time of the probe is about 1.5 microseconds on the proton channel. Therefore, a short delay, $\sim$2 μs, was put between each FSLG cycle with ^{1}H irradiation but not ^{15}N irradiation; this was found to be critical for achieving the theoretical scaling factor, because the rate of magnetization oscillation between ^{15}N and ^{1}H critically depends on the Hartmann–Hahn match condition (*29*). The zero-frequency intensity across the 2D contour plot (dipolar dimension) arises from the asymmetric approach to the equilibrium (*30*). This is possibly due to the proton spin-diffusion from the residual ^{1}H-^{1}H homonuclear interaction.

The observed distortions are due to partial orientation of the channel by the magnetic field resulting in an intensity contribution at $\sigma_{\|}$.

Spectra of a 2D PISEMA experiment on ^{15}N-Trp$_{13}$ gramicidin A in hydrated unoriented lipid bilayers at room temperature are shown in Fig. 3. Figure 3A is a 1D ^{15}N chemical-shift powder pattern; Fig. 3B is a contour plot of the 2D spectrum with the ^{15}N-^{1}H dipolar interaction in the F_1 dimension and the ^{15}N chemical shift in the F_2 dimension. As discussed above, the contour plot consists of two lines which intersect at the point where the dipolar splitting is zero, i.e., the channel axis is 54.7° with respect to the magnetic field. On the left, slices are taken along the dipolar interaction dimension corresponding to chemical shifts of 181.0, 103.0, and 67.0 ppm which represent the channel axis angles of 0, 54.7, and 90° relative to the magnetic field, respectively. The spectrum above the contour plot is the ^{15}N chemical-shift slice from the maximal dipolar splitting, corresponding to molecules with the channel axis aligned parallel to the magnetic field direction. The half-height linewidth of the resonance is about 8 ppm for the chemical-shift slice, and about 750 to 900 Hz for the dipolar splitting, corresponding to a ± 2–$4°$ error in the measured angle, ϑ. In comparison, the PISEMA experiment on oriented samples gives about 5 ppm in chemical-shift slices and about 600 Hz in dipolar splitting (data not shown).

As seen in Fig. 3B the ^{15}N-^{1}H dipolar splitting versus ^{15}N chemical shift is almost linear. The slope is about ± 270 Hz/ppm. Using previous determined values, $\beta = 17°$ and $\alpha = 0°$, $\sigma_{11} = -60$, $\sigma_{22} = -37$, and $\sigma_{33} = 98$ ppm (relative to $\sigma_{iso} = 0$ ppm) (*24*), and the dipolar coupling constant R = 11.335 kHz, based on an N-H bond length of 1.024 Å from neutron diffraction data (*25, 26*), the orientation of the channel axis in the PAS frame is determined to be $\zeta = 40.5 \pm 5°$, $\xi = 18.4 \pm 1°$, keeping in mind the ambiguity when interpreting the data, that four possibles solutions, $(\pm\zeta, \xi)$, $(\pi \pm \zeta, \pi - \xi)$ may be derived from the NMR data. The result is in good agreement with the calculated ζ and ξ from the known gramicidin A structure, which are 45.8° and 17.3°, respectively. Alternatively, if the PAS orientation to the rotational axis is known and the N-H vector is assumed to be in the peptide plane (i.e., $\alpha = 0°$), it is possible to calculate β, the angle between the N-H vector and σ_{33}.

The method demonstrated here provides a way to derive high-resolution structural information from a "powder" sample. For cases where oriented samples cannot be observed due to spectrometer hardware constraints, or where well-oriented samples have not been achieved, the measurements on unoriented samples might be the only way to get precise orientational constraints. For instance, oriented samples may become difficult to achieve when proteins have large extramembrane domains.

Another advantage is that this method is well suited for studying the anisotropy of the spin relaxation rates without resorting to single crystal or oriented samples, where a set of measurements are needed with samples oriented at different angles relative to the magnetic field direction (*27, 28*). Instead, these measurements can be accomplished simultaneously with a few two-dimensional experiments without sample rotation, since each cross peak in the 2D spectrum represents those molecules at a well-defined orientation. Moreover, the map of the anisotropic spin relaxation rates can be achieved with very high angular resolution.

ACKNOWLEDGMENTS

We are grateful to Dr. Stanley J. Opella and members of his group at the NIH Resource for Solid-State NMR of Proteins for useful discussions. The authors are indebted to the NMR facilities staff: R. Rosanske, T. Gedris, J. Vaughn, and A. Blue for their skillful maintenance and service of the NMR spectrometers and to H. Henricks and U. Goli in the Bioanalytical Synthesis and Services Facility for their expertise and maintenance of the ABI 430A peptide synthesizer and HPLC equipment. This work has been supported by NSF Grant DMB 9603935 and a portion of this work was performed at the National High Magnetic Field Laboratory supported by NSF Cooperative Agreement DMR-9527035 and the state of Florida.

REFERENCES

1. P. Palmas, P. Tekely, and D. Canet, Local-field measurements on powder samples from polarization inversion of the rare-spin magnetization, *J. Magn. Reson. A* **104,** 26–36 (1993).
2. J. Seelig, ^{31}P Nuclear magnetic resonance and the head group structure of phospholipids in membranes, *Biochim. Biophys. Acta* **515,** 105–140 (1978).
3. C. H. Wu, A. Ramamoorthy, and S. J. Opella, High-resolution heteronuclear dipolar solid-state NMR spectroscopy, *J. Magn. Reson. A* **109,** 270–272 (1994).
4. T. A. Cross and S. J. Opella, Solid-state NMR structural studies of peptides and proteins in membrane, *Curr. Opin. Struct. Biol.* **4,** 574–581 (1994).
5. R. R. Ketchem, W. Hu, and T. A. Cross, High-resolution conformation of gramicidin A in a lipid bilayer by solid-state NMR, *Science* **261,** 1457–1460 (1993).
6. R. R. Ketchem, B. Roux, and T. A. Cross, High-resolution polypeptide structure in a lamellar phase lipid environment from solid state NMR derived orientational constraints, *Structure* **5,** 1655–1669 (1997).
7. T. A. Cross, Structural biology of peptide and proteins in synthetic membrane environments by solid-state NMR spectroscopy, *Annu. Rep. NMR Spectrosc.* **29,** 124–158 (1994).
8. S. J. Opella, NMR and membrane proteins, *Nat. Struct. Biol.* **4, (Suppl.)** 845–848 (1997).
9. F. M. Marassi, A. Ramamoorthy, and S. J. Opella, Complete resolution of the solid state NMR spectrum of a uniformly ^{15}N-labeled membrane protein in phospholipid bilayers, *Proc. Natl. Acad. Sci. USA* **94,** 1739–1744 (1997).
10. Y. Kim, K. Valentine, S. J. Opella, S. L. Schendel, and W. A. Cramer, Solid-state NMR-studies of the membrane-bound closed state of the Colicin E1 channel domain in lipid bilayers, *Protein Sci.* **7,** 342–348 (1998).
11. F. D. Moll and T. A. Cross, Optimizing and characterizing alignment of oriented lipid bilayers containing gramicidin D, *Biophys. J.* **57,** 351–362 (1990).
12. S. Auge, H. Mazarguil, M. Tropis, and A. Milon, Preparation of

oriented lipid bilayer on ultrathin polymers for solid-state NMR analyses of peptide-membrane interactions, *J. Magn. Reson.* **124,** 455–458 (1997).

13. R. S. Prosser, S. A. Hunt, and R. R. Vold, Improving sensitivity in mechanically oriented phospholipid bilayers using ultrathin plates—A deuterium solid-state NMR study, *J. Magn. Reson. B* **109,** 109–111 (1995).
14. I. Sander and J. H. Prestegard, Magnetically orientable phospholipid bilayers containing small amounts of a bile salt analogue, CHAPSO, *Biophys. J.* **58,** 447–460 (1990).
15. R. S. Prosser, S. A. Hunt, J. A. DiNatale, and R. R. Vold, Magnetically aligned membrane model systems with positive order parameter: Switching the sign of S_{zz} with paramagnetic ions, *J. Am. Chem. Soc.* **118,** 269–270 (1996).
16. M. Lee and W. I. Goldburg, Nuclear-magnetic-resonance line narrowing by a rotating rf field, *Phys. Rev. A* **140,** 1261–1271 (1965).
17. A. Bielecki, A. C. Kolbert, and M. H. Levitt, Frequency-switched pulse sequences: Homonuclear decoupling and dilute spin NMR in solids, *Chem. Phys. Lett.* **155,** 341–346 (1989).
18. A. Bielecki, A. C. Kolbert, H. J. M. DE Groot, R. G. Griffin, and M. H. Levitt, Frequency-switched Lee–Goldburg sequences in solids, *Adv. Magn. Reson.* **14,** 111–124 (1990).
19. J. S. Waugh, Uncoupling of local field spectra in nuclear magnetic resonance: Determination of atomic positions in solids, *Proc. Natl. Acad. Sci. USA* **73,** 1394–1397 (1976).
20. O. S. Andersen, Gramicidin channels, *Ann. Rev. Physiol.* **46,** 531–548 (1984).
21. D. D. Busath, The use of physical methods in determining gramicidin channel structure and function, *Annu. Rev. Physiol.* **55,** 473–501 (1993).
22. K. C. Lee, W. Hu, and T. A. Cross, ^{2}H NMR determination of the global correlation time of the gramicidin channel in a lipid bilayer, *Biophys. J.* **65,** 1162–1167 (1993).
23. C. L. North and T. A. Cross, Correlations between function and dynamics: Time scale coincidence for ion translocation and molecular dynamics in the gramicidin channel backbone, *Biochemistry* **34,** 5883–5895 (1995).
24. W. Mai, W. Hu, C. Wang, and T. A. Cross, Orientational constraints as three-dimensional structural constraints from chemical shift anisotropy: The polypeptide backbone of gramicidin A in a lipid bilayer, *Protein Sci.* **2,** 532–542 (1993).
25. P. V. LoGrasso, L. K. Nicholson, and T. A. Cross, N-H bond length determinations and implications for the gramicidin channel conformation and dynamics from ^{15}N-^{1}H dipolar interaction, *J. Am. Chem. Soc.* **111,** 1910–1912 (1989).
26. A. Kvick, A. R. Al-Karaghouli, and T. F. Koetzle, Deformation electron density of α-glycylglycine at 82K. 1. The neutron diffraction study, *Acta Crystallogr. B* **33,** 3796–3801 (1977).
27. C. Mayer, G. Gröbner, K. Müller, K. Weisz, and G. Kothe, Orientation-dependent deuteron spin-lattice relaxation times in bilayer membranes: Characterization of the overall lipid motion, *Chem. Phys. Lett.* **165,** 155–161 (1990).
28. H. C. Jarrell, I. C. P. Smith, P. A. Jovall, H. H. Mantsch, and D. J. Siminovitch, Angular dependence of ^{2}H NMR relaxation rates in lipid bilayers, *J. Chem. Phys.* **88,** 1260–1263 (1987).
29. L. Müller, A. Kumar, T. Baumann, and R. R. Ernst, Transient oscillations in NMR cross-polarization experiments in solids, *Phys. Rev. Lett.* **32,** 1402–1406 (1974).
30. R. K. Hester, J. L. Ackerman, V. R. Cross, and J. S. Waugh, Resolved dipolar coupling spectra of dilute nuclear spins in solids, *Phys. Rev. Lett.* **34,** 993–995 (1975).